

## Mechanisms of Selective Antimicrobial Activity of Gaegurin 4

Heejeong Kim<sup>1,\*</sup>, Byeong Jae Lee<sup>2</sup>, Mun Han Lee<sup>1</sup>, Seong Geun Hong<sup>3</sup>, and Pan Dong Ryu<sup>1</sup>

<sup>1</sup>Laboratories of Veterinary Pharmacology and Biochemistry, College of Veterinary Medicine, <sup>2</sup>Laboratory of Molecular Genetics, Institute for Molecular Biology and Genetics and Department of Microbiology, Seoul National University, Seoul 151-742, <sup>3</sup>Department of Physiology, Institute of Health Sciences and Medical Research Center for Neural Dysfunction, College of Medicine, Gyeongsang National University, Jinju 660-751, Korea

Gaegurin 4 (GGN4), an antimicrobial peptide isolated from a Korean frog, is five times more potent against Gram-positive than Gram-negative bacteria, but has little hemolytic activity. To understand the mechanism of such cell selectivity, we examined GGN4-induced K<sup>+</sup> efflux from target cells, and membrane conductances in planar lipid bilayers. The K<sup>+</sup> efflux from Gram-positive *M. luteus* (2.5 µg/ml) was faster and larger than that from Gram-negative *E. coli* (75 µg/ml), while that from RBC was negligible even at higher concentration (100 µg/ml). GGN4 induced larger conductances in the planar bilayers which were formed with lipids extracted from Gram-positive *B. subtilis* than in those from *E. coli* ( $p < 0.01$ ), however, the effects of GGN4 were not selective in the bilayers formed with lipids from *E. coli* and red blood cells. Addition of an acidic phospholipid, phosphatidylserine to planar bilayers increased the GGN4-induced membrane conductance ( $p < 0.05$ ), but addition of phosphatidylcholine or cholesterol reduced it ( $p < 0.05$ ). Transmission electron microscopy revealed that GGN4 induced pore-like damages in *M. luteus* and dis-layering damages on the outer wall of *E. coli*. Taken together, the present results indicate that the selectivity of GGN4 toward Gram-positive over Gram-negative bacteria is due to negative surface charges, and interaction of GGN4 with outer walls. The selectivity toward bacteria over RBC is due to the presence of phosphatidylcholine and cholesterol, and the trans-bilayer lipid asymmetry in RBC. The results suggest that design of selective antimicrobial peptides should be based on the composition and topology of membrane lipids in the target cells.

**Key Words:** Antimicrobial peptide, Cell selectivity, Lipid composition, Planar lipid bilayer, K<sup>+</sup> efflux

### INTRODUCTION

Gaegurin 4 (GGN4) is one of 6 gaegurin peptides isolated from *Rana rugosa*, and consists of 37 amino acid residues with net 4 positive charges and one intra molecular disulfide bond on C-terminal 'rana box' (Park et al, 1994), which is a hepta peptide module conserved among antimicrobial peptides from the species in the genus, *Rana* (Morikawa et al, 1992; Simmaco et al, 1993; Clark et al, 1994; Park et al, 1994). Recently, esculantin-2EM has been suggested as new name of GGN4 (Won et al, 2009), according to the nomenclature suggested by Conlon (2008). GGN4 shows a broad-spectrum of antimicrobial activity against Gram-positive and Gram-negative bacteria, fungi and protozoa with little or no hemolytic activity at concentrations showing antimicrobial activity. Several lines of evidences indicate that the antimicrobial activity of GGN4 results from its pore-forming activity. For example, GGN4 forms cation-selective and voltage-dependent channels in lipid mem-

branes (Kim et al, 1999). Estimation of diameters of GGN4-induced pores by analytical ultracentrifugation indicates that GGN4-induced pores are composed of 5 GGN4 molecules or more with a diameter of 7.3 Å (Eun et al, 2006). The studies with nuclear magnetic resonance (NMR) spectroscopy also predicted the molecular structure of GGN4-induced pores and its shape (Chi et al, 2007; Park et al, 2007). The Rana box of GGN4 (C-terminal heptapeptide) is required for high ionophoric activity of GGN4, but does not participate in forming the pore (Kim et al, 2004). The disulfide bond, common to the 3<sup>rd</sup> group of Boman's classification of antimicrobial peptides (Boman, 2000) does not strongly affect the conformation and the antimicrobial activity (Park et al, 2000).

Antimicrobial activity of GGN4 is more potent against Gram-positive than Gram-negative bacteria, and respective minimum inhibitory concentrations (MIC) are 2.5 and 75 µg/ml. However, GGN4 does not affect RBC at this range of concentration (Park et al, 1994). In support of these findings, the ionophoric activity of GGN4 evaluated by measuring K<sup>+</sup> efflux is far more potent in Gram-positive bacteria than in Gram-negative bacteria or RBC (Kim et al, 2004).

**ABBREVIATIONS:** GGN4, gaegurin 4; RBC, red blood cell; PC, phosphatidylcholine; PE, phosphatidylethanolamine; PS, phosphatidylserine; CS, cholesterol; NMR, nuclear magnetic resonance.

Corresponding to: Pan Dong Ryu, Laboratory of Veterinary Pharmacology, College of Veterinary Medicine, Seoul National University, Seoul 151-742, Korea. (Tel) 82-2-880-1254, (Fax) 82-2-879-0378, (E-mail) pdryu@snu.ac.kr

\*Current address: Heejeong Kim, Redox Biology Center, Department of Biochemistry, University of Nebraska, Lincoln, Nebraska, USA.

However, little is known about the mechanisms of the selective toxicity of GGN4 against Gram-positive and Gram-negative bacteria, and RBC.

Human and other mammalian RBC membranes predominantly consist of zwitterionic lipids such as like phosphatidylcholine (PC), sphingomyelin, and phosphatidylethanolamine (PE). In contrast, bacterial membranes characteristically contain negatively charged lipids such as phosphatidylglycerol, and cardiolipin. Interestingly, Gram-positive bacterial membranes contain more negatively charged lipids and less neutral lipids compared to that of Gram-negative bacteria (Gennis, 1991). In addition, the abundance of cholesterol in RBC membranes and its absence in bacterial cells may underlie the different hemolytic activity of the peptides (Ames, 1968; Cronan & Roy, 1972; Gennis, 1991). For the antimicrobial peptides, it has been suggested that the selective activity of antimicrobial peptides is due to the differences in membrane lipid compositions of target cells (Matsuzaki et al, 1989; Zasloff, 2002; Gidalevitz et al, 2003; see for review Matsuzaki, 2009).

In this study, we hypothesized that the high sensitivity of Gram-positive bacteria and low sensitivity of Gram-negative bacteria and RBC to GGN4 is due to the differences in the lipid composition of cell membranes and/or wall. To test this hypothesis, we examined the pore forming activity of GGN4 by measuring GGN4-induced conductances in the planar lipid bilayers, and GGN4-induced K<sup>+</sup> efflux from bacteria and RBC. We also examined morphological changes of bacterial cell membranes when treated with GGN4 using transmission electron microscopy.

## METHODS

### *Planar lipid bilayers*

Planar lipid bilayers (Kim et al, 1999) were formed by painting lipid solution over an aperture (200 μM) of a plastic cup (0.6 ml) using a fire-polished glass rod in a buffer containing 10 mM N-(2-hydroxyethyl)piperazine-N'-(2-ethanesulfonic acid) (HEPES) adjusted to 7.4 with 1 M N-methyl d-glucamine (NMDG) or KOH. Lipid solutions were made by a mixture of phospholipids, cholesterol, or extracted lipids at a certain proportion of each lipid in n-decane (25 mg/ml).

Formation of the bilayers was visualized on an oscilloscope screen as increase of membrane capacitances while applying a triangular wave under voltage clamp. The final capacitances of the membranes ranged from 100 to 200 pF. When the leak current was larger than 1 pA at 100 mV, a new membrane was formed. The final salt concentrations were adjusted by adding an appropriate amount of 3 M KCl to the front compartment of the recording chamber (1.2 ml, designated as "cis" compartment). A small amount (1~5 μl) of the stock peptide (45 or 450 μg/ml) was added to the cis chamber and the solution was stirred with a small magnet bar (1×3 mm). The final concentrations of GGN4 were in the range of 0.01~5 μg/ml (2.7~1,350 nM). Formation of the pores (channels) was identified as an abrupt shift or appearance of the gating-like fluctuation of the current trace from an oscilloscope screen.

### *Electrical measurement and data analysis*

GGN4-induced currents were measured at steady voltage or ramp voltage command by using an amplifier designed

for bilayer experiments (BC525A, Warner Instr. Co., Hamden CT, USA; Park et al, 2003). The amplifier headstage was connected to the bath via an agar (3%) bridge to reduce junction potentials. Electrode asymmetry was corrected at symmetrical salt condition before formation of the bilayers. GGN4-induced currents were directly stored on a personal computer using a Digidata 1,200 data acquisition unit (Axon Instrument. Co., Foster City, CA, USA), VTR tapes using a VR-10 digital data recorder (Instrutech Corp., New York, NY, USA), and also recorded on a pen recorder. We used a software, pClamp (Version 6.03, Axon Instrument. Co., Foster City, CA, USA) for voltage command, and measurement of current amplitudes and reversal potentials. The data were presented as mean±standard error of mean. By convention, we designated the compartment we added the peptide as "cis" and the other as "trans" compartment. Membrane potential was defined as that of the cis compartment with respect to that of the trans compartment, and the current flow from cis to trans compartment as "outward current". The current-voltage relations were obtained either by measuring the amplitude of unitary conductance of GGN4-induced current, or by applying a ramp voltage command from -80 to +80 mV or from +80 to -80 mV for 3 seconds. In particular, since the lifetime of the bilayers formed with extracted lipids (in particular, *Bacillus subtilis*) was very short (<1 min) in the presence of GGN4, it was difficult to measure the conductances for multiple GGN4 concentrations using 100 mM KCl ion salt solution. Therefore, the membrane conductances at a single concentration of GGN4 were measured in given membranes formed with extracted lipids in 25 mM KCl solution. GGN4-induced conductances usually reached a steady-state at 7~10 min after the addition of GGN4. Therefore, we applied the ramp pulses after a 10 min of continuous stirring. The membrane conductance (g) was obtained from current-voltage relations by Ohm's law,  $g=I/V$ , in which I is current and V is voltage. The single channel data were filtered at 500 Hz (-3 dB, corner frequency, 8-pole Bessel filter) and digitized at a sampling rate of 2 kHz.

### *Measurement of K<sup>+</sup> efflux from bacteria and human RBC*

*Micrococcus luteus* (*M. luteus*, ATCC4698) and *Escherichia coli* (*E. coli*, JM109) were grown to the mid-logarithmic growth phase at 37°C in a medium containing bacto-tryptone (1%), yeast extract (0.5%), and NaCl (0.5%). The cells were washed three times with an incubation solution containing 0.15 M NaCl, and 10 mM HEPES-NaOH (pH 7.0, 37°C), and then resuspended in the same buffer at 10<sup>8</sup> cfu/ml. The K<sup>+</sup> efflux from the cells was monitored by a K<sup>+</sup> ion-selective electrode (Phoenix Co.) connected to an ion meter at 22~24°C. The electrode exhibits a Nernstian response (53 mV/decade) from 10<sup>-5</sup> to 10<sup>-3</sup> M. The cell viability was also determined during K<sup>+</sup> efflux experiment. Briefly, bacterial samples were taken at fixed intervals, diluted with the incubation solution and dispersed on a Luria Bertani agar medium. The viability of bacterial cells was determined by counting colonies after 1 day of incubation at 37°C. RBCs were isolated from human blood treated with heparin by centrifuging for 10 min at 1,000 g. Cells were washed twice with a solution containing 0.15 M NaCl, 10 mM HEPES, and 1 mM EDTA (pH 7.4) and suspended at a concentration of 1% (v/v). Total amount of K<sup>+</sup> efflux from both bacteria and RBCs was determined by disrupting cells with 0.5% Triton X-100.

### Purification of bacterial and RBC membrane lipids

Bacterial membrane lipids were extracted and purified by modified method of Ames (1968). *E. coli* (JM109) or *B. subtilis* (KCTC1021) cells (300 g, wet weight) were resuspended by homogenization in 347 ml of distilled water. From this step on, all operations were performed under an atmosphere of nitrogen and protected from light. The homogenized cells were transferred to a glass-stoppered bottle and stirred with a magnetic bar, and chloroform (0.7 L) and methanol (1.4 L) were then added and stirred for 12 hr. Particulate debris were removed from the extract by centrifugation at 900 g for 15 min and the clear supernatant was collected. Lipids were separated from water-soluble substances by sequential addition of chloroform (645 ml) and distilled water (645 ml). Then, the mixture was stirred for 3 hr at room temperature. The magnetic stirrer was turned off in order to allow the extract to settle and partition into 3 distinct layers: an upper phase consisting of methanol-water, a brown particulate inter-phase, and a lower layer of chloroform. The chloroform phase was carefully recovered and evaporated to dryness in a rotary evaporator at 30°C. The dried residue was stored at -70°C.

Membrane lipids of RBC were extracted by the procedures of Agre and Bennett (1988). RBCs were separated from platelet rich plasma by centrifugation (180 g, 20 min, 22°C), and washed three times with a citrate/saline buffer. The ghosts of RBC (100 to 200 ml) were prepared by hypotonic lysis (7.5 mM NaH<sub>2</sub>PO<sub>4</sub>, 1 mM EDTA, pH 7.5) of washed RBCs. Contaminated leukocytes and platelets that were resistant to lysis were removed by discarding the small thick white pellet under the fluffy red cell ghost layer after each centrifugation. Washed RBC ghosts were extracted with solvent mixture (Ghosts : H<sub>2</sub>O : MeOH : CHCl<sub>3</sub>, 1 : 3 : 10 : 5, v/v/v/v) by stirring for 30 min at 22°C, and the extract was dried with a rotary evaporator and stored at -70°C.

Total lipid phosphorus was assayed by the modified Ames method (Lau et al, 1979). Briefly, to 0.01~0.1 ml of phosphate sample in a Pyrex test tube was added 50 μl of 10% Mg (NO<sub>3</sub>)<sub>2</sub> in 95% alcohol. The mixture was dried and shed by shaking the tube over a strong flame until brown fumes disappeared. The tube was then allowed to cool, and 0.3 ml of 0.5 N HCl was added. The tube was heated in a boiling water bath for 15 min to hydrolyze the pyrophosphate formed in ash to phosphate. Cooling the tops of the tubes by a stream of air helped to minimize evaporation. After the tube was cooled, 0.7 ml of a mixture (10% ascorbate: 0.42% molybdate, 1 : 6, v/v) was added, and the tubes were incubated for 20 min at 45°C and read at 820 nm. The phosphorus contents were calculated by a calibration curve obtained using KH<sub>2</sub>PO<sub>4</sub>.

### Transmission electron microscopy

*M. luteus* and *E. coli* cells were prepared as described in K<sup>+</sup> efflux study. *M. luteus* and *E. coli* of 10<sup>8</sup> cfu/ml were incubated with GGN4 for 30 min at their MIC levels (2.5 μg/ml for *M. luteus* & 75 μg/ml for *E. coli*). After incubation, bacterial cells were fixed in a modified Karnovsky's fixative (Kim & Fulton, 1984), consisting of 2% glutaraldehyde and 2% paraformaldehyde in 50 mM sodium cacodylate buffer (pH 7.2), for 2 h at room temperature under a low vacuum. The specimens were rinsed twice with the same buffer and postfixed in 1% osmiumtetr-

oxide for 2 h, *en bloc* stained overnight in 0.5% aqueous uranyl acetate at 4°C, and dehydrated in an ethanol series before they were embedded in Spurr's low viscosity medium. Embedded samples were sectioned with a diamond knife and double stained with 2% aqueous uranyl acetate for 5 min and lead acetate before examination under a JEOL1010 electron microscope (Tokyo, Japan). Experiments were repeated at least five times with different samples for both bacteria.

### Chemicals

Natural gaegurin 4 was purified from the skin of frogs as described previously, and the purity (>99.9%) was confirmed by analytical HPLC (Park et al, 1994). Synthetic GGN4 (MW 3,748) was purchased from American Peptide Co. (Sunnyvale, CA, USA). The peptide purity determined by reverse phase HPLC and MASS spectrometry was >99.9%. Synthetic phospholipids such as palmitoyloleoyl phosphatidylethanolamine (PE), palmitoyloleoyl phosphatidylcholine (PC), and palmitoyloleoyl phosphatidylserine (PS) were purchased from Avanti Polar Lipids (Alabaster, AL, USA). All other reagents were of highest analytical grade purchased from Aldrich Chemical Co. (Milwaukee, WI, USA) or Sigma Chemical Co. (St. Louis, MO, USA).

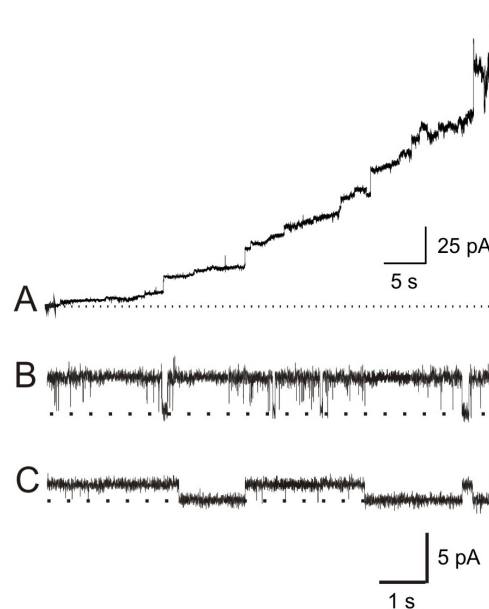


**Fig. 1.** GGN4-induced membrane currents. (A) Induction of membrane conductance by GGN4 (0.3 μg/ml). Current record shows the changes in membrane conductances induced by GGN4 in a lipid bilayer, composed of PE : PS (1 : 1), under 200/0 (*cis/trans*) mM KCl gradient at 0 mV in the recording solution containing 10 mM HEPES-NMDG (pH 7.2). (B and C) Typical records showing unitary conductances of GGN4 (0.03 μg/ml)-induced pores at symmetrical 100 mM KCl in acidic (PE : PS=3 : 7, B) and neutral lipid membranes (PE 100%, C) at 30 mV.

## RESULTS

### Heterogeneous membrane conductances-induced by GGN4 in planar lipid bilayers

As reported previously (Kim et al, 1999), GGN4 (0.01~1  $\mu\text{g}/\text{ml}$ ) induced membrane currents immediately after applying it to planar lipid membranes. Fig. 1A shows typical example of the membrane conductances induced by GGN4 (0.3  $\mu\text{g}/\text{ml}$ ) in planar lipid bilayer formed with PE : PS (1 : 1) under asymmetric condition (200/0 mM KCl). The conductances continued to increase, and eventually membranes were broken up in the presence of GGN4. In the absence of GGN4, such membrane conductances were not observed (data not shown). GGN4-induced channels were heterogeneous in their conductance and gating. In about half of bilayers tested, GGN4 induced discrete gating-like activities with fixed conductance levels (Fig. 1B and 1C), whereas GGN4 induced conductances appeared like a simple leakage or erratic fluctuations in other half of membranes.

### GGN4-induced $\text{K}^+$ efflux from bacteria and human RBCs

Efflux of intracellular  $\text{K}^+$  ions is commonly used to evaluate the ability of pore-forming antimicrobial peptides (Orlov et al, 2002). To compare the channel forming ability of GGN4 directly in living cells, we examined  $\text{K}^+$  efflux from Gram-positive (*M. luteus*) and Gram-negative bacteria (*E. coli*), and RBC (Fig. 2). Fig. 2A shows that GGN4 induced  $\text{K}^+$  efflux from *M. luteus* in a concentration-dependent manner. At 0.5  $\mu\text{g}/\text{ml}$ , GGN4 induced little  $\text{K}^+$  accumulation from *M. luteus*, however, the peptide induced a rapid and concentration-dependent  $\text{K}^+$  efflux at 2.5 and 12.5  $\mu\text{g}/\text{ml}$

and reached a steady state within 2 min. The time to steady-state was faster, and the level of steady state of  $\text{K}^+$  efflux was higher with increasing GGN4 from 2.5 to 12.5  $\mu\text{g}/\text{ml}$ . In addition, the viability of *M. luteus* rapidly reduced to below 50% within 5 min (Fig. 2D). In contrast, the  $\text{K}^+$  efflux from *E. coli* was not observed at 2.5  $\mu\text{g}/\text{ml}$ , and a noticeable  $\text{K}^+$  efflux was observed at 75  $\mu\text{g}/\text{ml}$ , which is equivalent to the MIC of GGN4 to *E. coli*. In addition, the time to steady state is far slower (~30 min, not illustrated) than that in *M. luteus* (Fig. 2B). The efflux of  $\text{K}^+$  from human RBC was not observed at 2.5  $\mu\text{g}/\text{ml}$ , and a weak and slow  $\text{K}^+$  efflux was observed at 100  $\mu\text{g}/\text{ml}$ . The GGN4-induced  $\text{K}^+$  efflux from RBC was below 10% of total amount of  $\text{K}^+$  even at 50 min after application of GGN4. Collectively, these results suggest that the ionophoric ability of GGN4 is closely correlated with its antimicrobial activity in live cells.

### Effect of membrane lipids extracted from bacterial and RBC cells on GGN4-induced membrane conductances

To determine whether cell selectivity of GGN4 is related to membrane lipid composition of target cells, we formed planar lipid bilayers with lipids extracted from target cells such as *B. subtilis*, *E. coli*, and human RBC, and tested its ionophoric activity. GGN4 (0.03  $\mu\text{g}/\text{ml}$ ) readily induced the currents within 2~4 min in membranes formed with lipids extracted from *B. subtilis* (Fig. 3A). Once the conductance started to increase, the currents continued to increase and the bilayer was eventually disrupted. However, for the membranes formed with lipids extracted from *E. coli*, the same concentration of GGN4 produced little change in the membrane conductance, and higher concentrations of GGN4 were required to induce channel-like activities. Even with higher concentration of GGN4 (0.1  $\mu\text{g}/\text{ml}$ ), the

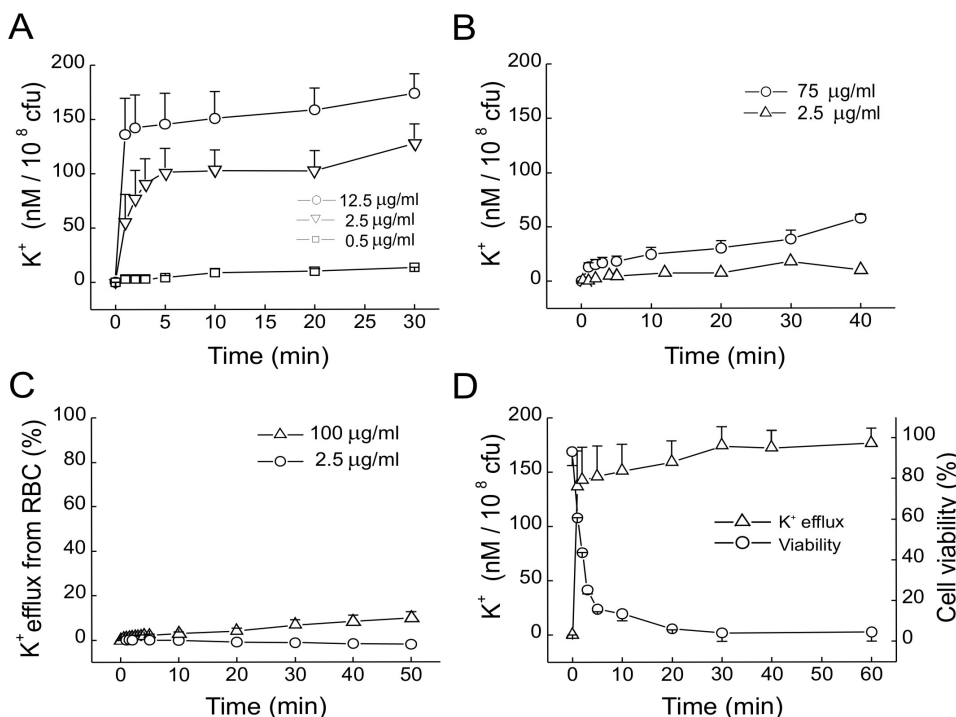


**Fig. 2.** Effects of GGN4 on  $\text{K}^+$  efflux from bacteria and RBC in the solution containing 10 mM HEPES-NaOH (pH 7.0) and 0.15 M NaCl. (A-C)  $\text{K}^+$  efflux from *M. luteus* (A), *E. coli* (B), and RBC (1%, v/v) in the presence of GGN4 (C). (D) Time courses of  $\text{K}^+$  efflux ( $\Delta$ ) and cell viability ( $\circ$ ) after application of GGN4 (12.5  $\mu\text{g}/\text{ml}$ ) to *M. luteus* suspension. The extent of  $\text{K}^+$  efflux was normalized to the total  $\text{K}^+$  efflux obtained after treatment with 0.5% Triton X-100.

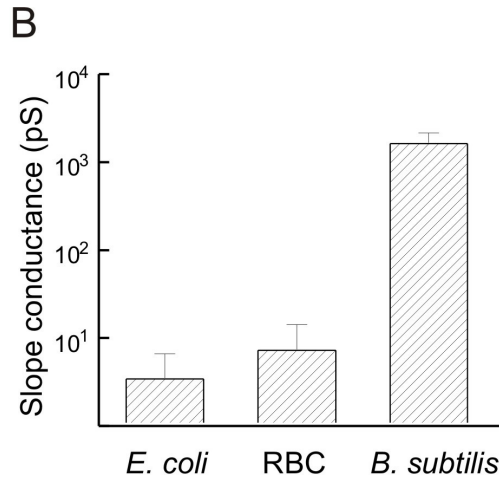
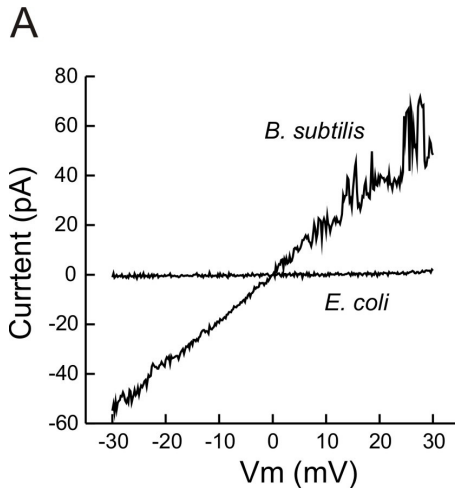


**Fig. 3.** Pore-forming activity of GGN 4 in the membranes formed with lipids extracted from G(+), Gram-negative bacteria and RBC in symmetric 25 mM KCl. (A) Current-voltage relation of GGN4-induced channels in the membranes formed with the extracted lipids in response to a ramp pulse (0.03  $\mu$ g/ml in *E. coli* lipid membrane and 0.1  $\mu$ g/ml in *B. subtilis* lipid membrane). (B) Mean slope conductances of the membranes formed with lipids extracted from *B. subtilis*, *E. coli* and RBC. Bars represent standard error of means.  $n=6$ .

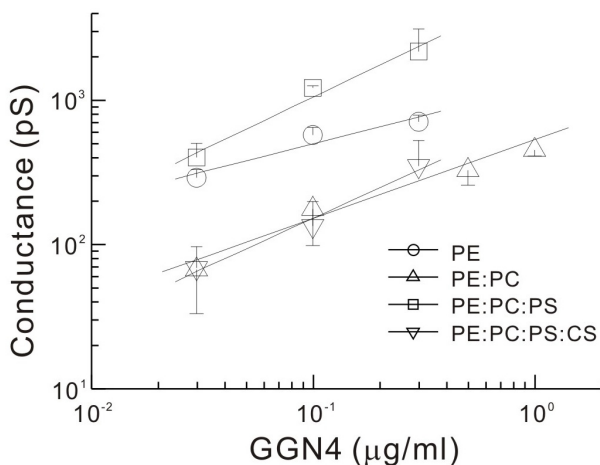


**Fig. 4.** Effects of addition of PC, PS and cholesterol to the lipid bilayers on GGN4-induced conductances. Slope conductances of the membrane at each GGN4 concentration were estimated from the current-voltage relations as shown in Fig. 3. Solid lines are drawn by the linear regression of double logarithmic concentration-conductance relations. Respective slopes of log space (conductance, pS) vs. log. (concentration,  $\mu$ g/ml) are 0.391, 0.546, 0.738 and 0.704 for PE, PE : PC, PE : PC : PS, and PE : PC : PS : CS membranes, respectively. PE, 100% phosphatidylethanolamine; PE : PC, 80% phosphatidylethanolamine and 20% phosphatidylcholine; PE : PC : PS, 80% phosphatidylethanolamine, 10% phosphatidylcholine and 10% phosphatidylserine; PE : PC : PS : CS, 50% phosphatidylethanolamine, 10% phosphatidylcholine, 10% phosphatidylserine, and 30% cholesterol. Symbols and bars represent the means and error bars of slope conductances, respectively, measured from 3~6 bilayers, except the data point at 0.3  $\mu$ g/ml in PE : PC : PS : CS membrane, where  $n=2$ .

conductances were smaller than those induced by GGN4 (0.03  $\mu$ g/ml) on bilayers of *B. subtilis* membranes at +30 mV. The effects of GGN4 on RBC membranes were similar to those on *E. coli* membranes (not illustrated). The mean slope conductances induced by GGN4 in lipid bilayers from *B. subtilis* were more than 100 times larger than those from

*E. coli* or RBC (Fig. 3B, 1,660 vs. 3.5~10 pS,  $n=6$ ;  $p<0.01$ ).

#### Effects of synthetic membrane lipids on the GGN4-induced membrane conductances

To further examine the effects of membrane lipids on ionophoric activity of GGN4, we measured GGN4-induced conductances in the membranes containing various synthetic lipids such as PC, PS and cholesterol (Fig. 4, symbols). Addition of PC (30%) reduced the slope conductance induced by GGN4 (0.03~0.3  $\mu$ g/ml) to one third to one fifth of that in PE (100%;  $568\pm74$  pS,  $n=4$  vs.  $175\pm77$  pS,  $n=3$ ,  $p<0.01$ , at 0.1  $\mu$ g/ml). The GGN4-induced slope conductances in PC containing membranes were significantly smaller than those in pure PE membranes at all three concentrations tested ( $p<0.01$ ,  $n=3$  for PE and 4 for PE : PC membranes). In contrast, addition of PS to PE : PC membranes significantly increased the GGN4-induced slope conductance by 6~7 folds ( $175\pm77$  pS,  $n=3$  vs.  $1,202\pm42$  pS,  $n=3$ ;  $p<0.01$ , at 0.1  $\mu$ g/ml). As shown in Fig. 1C, the GGN4-induced unitary conductances in PS containing membranes are also larger than those in neutral PE membranes. Mean amplitude of the unitary currents in 70% PS membranes was approximately 2 times larger than that in PE membranes ( $151.85\pm30.02$  pS,  $n=14$  vs.  $63.45\pm11.4$  pS,  $n=11$ ;  $p<0.05$ ). Addition of cholesterol (CS) to PE : PC : PS membrane again significantly reduced the GGN4-induced membrane conductances to about one sixth ( $1202\pm42$  pS,  $n=3$  vs.  $133\pm64$  pS,  $n=5$ ;  $p<0.001$ , at 0.1  $\mu$ g/ml). As shown in Fig. 4, the concentration-conductance relations were linear in double logarithmic curves (solid lines) and grossly parallel. The slope values ranged from 0.391 to 0.738 with the correlation coefficients of 0.964~0.999. Addition of PC increased the slope of the concentration-conductance relation curves from 0.391 to 0.546, while reducing the ionophoric effect of GGN4. Addition of PS increased the slope from 0.546 to 0.738, while increasing the ionophoric effect of GGN4. However, addition of CS did not significantly change the slope of the double-logarithmic curves of concentration-conductance relations although the GGN4-induced conductances were reduced (0.738 vs. 0.704).

### Damages on membranes of bacteria when treated with GGN4

In order to directly visualize the effect of GGN4 on the bacterial membranes, we examined the GGN4-induced morphological changes by transmission electron microscopy in Gram-positive and Gram-negative bacteria after treatment with at 2.5 and 75  $\mu\text{g/ml}$  GGN4 for 30 min; the concentrations of GGN4 found to induce  $\text{K}^+$ -efflux (see Fig. 2). The untreated *M. luteus* cells (230~916 nm in diameter) showed dark cytoplasm with smooth wall (~34 nm, Fig. 5A), whereas the treated cells showed obvious disruptions of different length in the bacterial wall and/or membrane (arrows in Fig. 5B; 55, 125, 263 nm) and less dark cytoplasm. The bacterial cells showing such changes are mostly at diploid stage. Fig. 5C illustrates the bacterial cytoplasm being leaked out through a pore (~55 nm in diameter) in a diploid bacteria, which still has considerable elec-

tronic density (Fig. 5C). Damaged cells also showed a region of low electronic density filled with fibrillary structures and small spots of higher electronic density in the cytoplasm. The cytoplasmic contents were heavily depleted in some cells. The untreated *E. coli* cells of cross (~625 nm) or horizontal sections (~2,420 nm) had dark cytoplasm and rough walls (~32 nm). The treated *E. coli* cells showed lower electronic density than the untreated *E. coli* (Fig. 5 D and E). Numerous long bleb-like structures were found, and some of them continued from the outer wall of the *E. coli* cells (arrows, Fig. 5E), indicating that outer walls of *E. coli* cells are separated by layer by layer from the cell body. The obvious deformity was rarely observed in the inner membranes of *E. coli*. Fig. 5F illustrates a space developing between outer wall and inner membrane of an *E. coli* cell at an area affected by GGN4. In addition, the localized spots of higher electronic density were also observed within the cytoplasm of an affected *E. coli*.

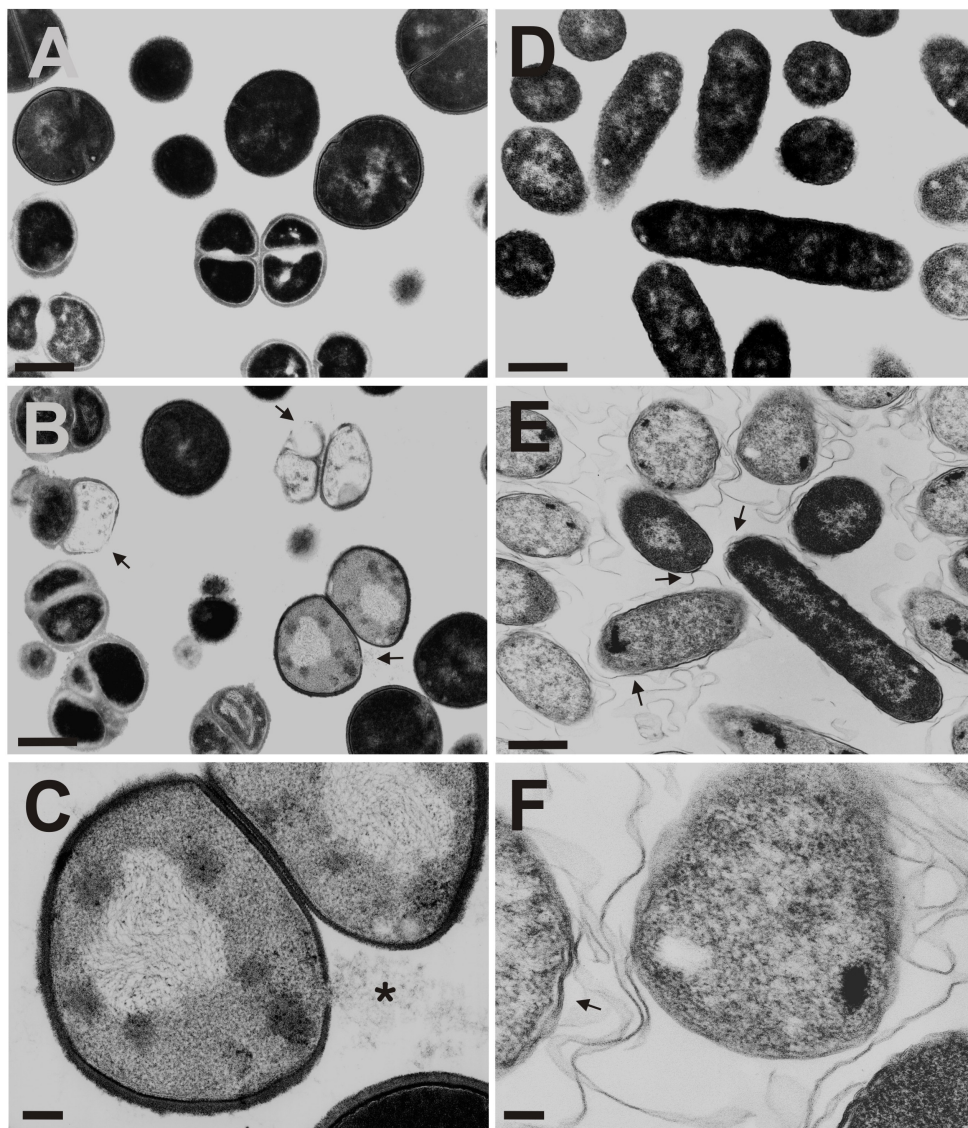


**Fig. 5.** Transmission electron micrographs of *M. luteus* and *E. coli* treated with GGN4 at 37°C for 30 min. *M. luteus* and *E. coli* cells ( $10^8 \text{ cfu/ml}$ ) were incubated with 2.5 and 75  $\mu\text{g/ml}$  GGN4, respectively. (A-C) Transmission electron micrographs of *M. luteus* untreated (A) and treated with GGN4 (B and C). Note the pores (marked by arrows) on the bacterial membranes (B). One of the pores shown in (B) was illustrated at higher magnification to show cytoplasm leaking out through the pore of about 55 nm (marked by \*, C). (D-F) Transmission electron micrographs of *E. coli* untreated (D) and treated with GGN4 (E and F). Note the layers of outer wall debris were peeled off from the damaged membranes (arrows) and a space developed between outer wall and inner membrane of *E. coli* at a damaged site (E, arrow). The bars represent 0.5  $\mu\text{m}$  for (A), (B), (D) and (E), and 0.1  $\mu\text{m}$  for (C) and (F).

## DISCUSSION

This study shows the mechanisms of selective actions of GGN4 toward Gram-positive bacteria over Gram-negative bacteria, or toward bacterial cells over RBC. We found that such selective activity of GGN4 is likely due to the differences in the property of phospholipids in the membranes and the topology of phospholipids.

### **Mechanisms of selective activity of GGN4 on Gram-positive over Gram-negative bacteria**

In this study, GGN4-induced  $K^+$  efflux was much less in RBC than that in Gram-positive and Gram-negative bacteria at respective MIC levels (2.5 and 75  $\mu\text{g/ml}$ , Park et al, 1994). GGN4 also induced a significantly higher membrane conductance ( $>\times 400$ ) in the bilayers formed with lipids from Gram-positive bacteria than in the bilayers from Gram-negative bacteria (Fig. 4). These findings are in good agreement with its antimicrobial activity (Park et al, 1994), and suggest that the selective activity of GGN4 against Gram-positive bacteria could be due to the differences in the property of lipid membranes. In view of the fact that GGN4 has net 4 positive charges (Park et al, 1994), it is likely that GGN4 preferentially binds to negatively charged lipids compared with zwitterionic phospholipids such as PE. This idea is supported by our present findings that pore forming ability of GGN4 was more pronounced in negatively charged membranes (larger slope conductances and unitary currents) than neutral lipid membranes. This observation is also in agreement in part with Park et al. (2003), who showed that the ionic currents through  $\text{Ca}^{2+}$ -activated  $K^+$  channels are larger in the planar lipid bilayers containing acidic phospholipids such as PS or phosphatidylinositol. The findings that addition of PS to the planar bilayers increased the slope of double logarithmic concentration-conductance curves (from 0.391 to 0.738) also indicate that more peptides are involved in the ionophoric activity in the bilayers containing PS (Kagan et al, 1990).

It is known that the portions of negatively charged lipids such as phosphatidylglycerol and cardiolipin are rich in *B. subtilis* membranes (70~80%; Bishop et al, 1967; Clejan et al, 1986), but low in the membranes of *E. coli* cells (17~26%; Bishop et al, 1973; Morein et al, 1996). Therefore, the higher ionophoric activity of GGN4 in the bilayers formed with the lipids from Gram-positive bacteria, *B. subtilis*, is likely due to a stronger electrostatic interaction of positive charges in GGN4 molecules and negative surface charges on the planar lipid bilayers (Dathe et al, 1996). These results also indicate that GGN4 belongs to the family of antimicrobial peptides such as magainin, cecropins, and dermaseptins, which have positive charges and hydrophobicity, and are selective toward bacteria (see for reviews, Matsuzaki, 1999; Shai, 2002).

The transmission electron micrographs of treated bacteria also indicated that the mode of antibacterial effects of GGN4 is different between Gram-positive and Gram-negative bacteria. A 30 min-treatment of GGN4 at MIC induced pore-like discontinuity in both inner and outer membranes of Gram-positive bacteria. Damaged *M. luteus* cells were mostly at diploid states. This might be due to the presence of lipid domains rich in acidic phospholipids, such as cardiolipin, in bacterial cell division (Dowhan, 1997; Matsumoto et al, 2006). However, the mechanism of such high sensitivity of diploid Gram-positive bacteria remains

to be studied further. In *E. coli*, the pore-like membrane damages were not obviously observed in the inner membranes, but a large part of the outer membrane in each cells was separated from the inner membranes in most cells affected. Such changes in the outer membranes seem to be different from the peptide-induced blebs observed in *E. coli* when treated with cecropin B or synthetic antimicrobial peptides (Shai, 2002), because the membrane debris were waved, and did not form any closed space in GGN4-treated *E. coli* cells. These results suggest that linear GGN4 almost simultaneously acts on both inner and outer membranes in Gram-positive bacteria, but acts on the outer membrane first and on the inner membrane with a delay in Gram-negative bacteria. The mode of action of GGN4 in Gram-negative bacteria seems to be different from magainin 2, a 23 antimicrobial peptide from frog, in that cyclic magainin 2 is less active than linear form because the cyclic peptides are bulky and interact with outer membrane lipids such as lipopolysaccharides in Gram-negative bacteria and teichoic acids in Gram-positive bacteria (Shai, 2002). Therefore, one could expect an interaction of GGN4 with these outer wall lipids by electrostatic interactions, but whether GGN4, which is larger than magainin 2 (23 vs. 37 amino acids), acts as linear or aggregated form remains to be further studied.

### **Mechanisms of selective activity of GGN4 on bacteria over RBC**

In the present study, the selective activity of GGN4 for bacterial cells over RBC was also confirmed. GGN4 induced much less  $K^+$  efflux in RBC than in Gram-positive or Gram-negative bacteria. Such selectivity could be due to the differences in membrane properties such as surface charge, head group of phospholipids, and presence of cholesterol. Firstly, the selective activity of GGN4 may be due to PC present in the human RBC membrane. Human RBC is composed of PE, PC, PS, and sphingomylein (22, 25, 10, 18%), whereas bacterial membranes do not contain PC (Bishop et al, 1967; Bishop et al, 1973; Clejan et al, 1986; Gennis, 1991; Morein et al, 1996). In this study, GGN4-induced conductance in PC containing membranes was significantly smaller than that in pure PE membranes, indicating that the selective activity of GGN4 could be due, in part, to PC in RBC membranes. The slope of double logarithmic curve of concentration-conductance curves was increased from 0.391 to 0.546 at concentrations of 0.03~0.1  $\mu\text{g/ml}$ , indicating an increase in the number of GGN4 molecules associated with bilayers.

Although both PC and PE have a net neutral charge, PE and PC are not exchangeable in their response to electrochemical potential, because only PE can make hydrogen bond (Dowhan, 1997) indicating that GGN4 can discriminate PE membranes from PC containing membranes and this ability of GGN4 may play a role in its selective toxicity. However, further study is needed to clearly understand the molecular behaviors of GGN4 in the bilayers which are formed with PE alone or PE and PC. Secondly, the selective activity of GGN4 may be due to the smaller portion of acidic phospholipids in the human RBC membrane. As discussed above, the smaller amount of acidic phospholipids in RBC (10%) is responsible for the smaller ionophoric activity of GGN4 in RBC than in *E. coli* (17~26%) or in *B. subtilis* (70~80%). Another factor is the transbilayer asymmetry of membrane phospholipids; the acidic phospholipid, PS

(10%), is not present on the outer leaflet, but on the inner leaflet of the bilayer of human RBC, therefore, one cannot expect any substantial electrostatic interaction between GGN4 and bilayers (Balasubramanian & Schroit, 2003; Daleke, 2008). In the experiments with the extracted lipids, we observed that the ionophoric effects of GGN4 in the planar lipid bilayers formed with RBC lipids were not smaller, but even higher than those in planar lipid bilayers formed with *E. coli* lipids. These results are different from the results showing selective activity on bacterial cells in live bacterial and RBC cells (Fig. 2; Park et al, 2004), and likely due to the disruption of transbilayer asymmetry of phospholipids in RBC under our experimental conditions. Thirdly, the selective activity of GGN4 may be due to cholesterol present in the human RBC membrane. This idea is supported by the facts that cholesterol is present in human RBC membranes (~25%), but absent in bacterial membranes (Gennis, 1991), and that the ionophoric activity of GGN4 was reduced by 6~7 folds in the planar lipid bilayers containing cholesterol (30%, Fig. 4). Our results are consistent with the report on the effects of magainin on RBC and sterol-containing membranes (Matsuzaki et al, 1995). The reduced activity of GGN4 on the membranes containing cholesterol could be due to the membrane rigidity induced by cholesterol (Bloch, 1991), the stabilization of lipid bilayer and reduced interactions between cholesterol and the peptide (Matsuzaki, 1999). However, in the experiments with the extracted lipids from human RBC (Fig. 3), the ionophoric activity of GGN4 was not smaller, but even larger in the bilayers formed with RBC membranes than in the bilayers formed with *E. coli* membrane. These results are not consistent with the results, based on K<sup>+</sup>-efflux or slope conductances in synthetic bilayers. Presently, we do not have any good explanation of why the effect of GGN4 was not reduced in the bilayers formed with lipids extracted from RBC, which are known to contain cholesterol (~25%). In addition, the slope of double logarithmic curve of concentration-conductance relations was increased in the bilayers containing either PC or PS, but not changed in the bilayers containing cholesterol, indicating that the presence of cholesterol does not significantly affect the cooperativity in GGN4-bilayer association (Kagan et al, 1990).

Taken together, GGN4-induced K<sup>+</sup> efflux is closely correlated with its antimicrobial activity. The selective activity of GGN4 toward Gram-positive over Gram-negative bacteria may arise from the high level of acidic phospholipids in the Gram-positive bacteria, and the fact that the outer wall of Gram-negative bacteria functions as a barrier for inner phospholipid membranes. In addition, GGN4 induces a pore-like damage across both outer wall and phospholipids membranes in Gram-positive bacteria, however, a dis-layering damage on the outer wall in Gram-negative bacteria. The selective activity of GGN4 toward bacteria over RBC may arise from a stability induced by PC and cholesterol that are present only in the mammalian cells, and from the trans-membrane lipid asymmetry that keeps acidic phospholipids in the inner leaflet of the membranes. Our results indicate that the selective activity of GGN4 is largely dependent on the composition and topology of lipids in bacteria and mammalian cell membranes. The peptide-lipid interactions observed in this study are expected to be valuable clues in designing of antimicrobial peptides with high cell selectivity.

## ACKNOWLEDGEMENTS

Authors like to thank Dr Jang Won Yoon for technical assistance in K<sup>+</sup> efflux experiments and Dr So Yeong Lee for critical reading of the manuscript. This work was supported by KOSEF 96-04-03-C.

## REFERENCES

- Agre P, Bennett V. Qualitative and functional analyses of spectrin, ankyrin, band 3, and calmodulin in human red cell membranes. *Methods Hematol* 19: 95–98, 1988
- Ames GF. Lipids of *Salmonella typhimurium* and *Escherichia coli*: structure and metabolism. *J Bacteriol* 95: 833–843, 1968
- Balasubramanian K, Schroit AJ. Aminophospholipid asymmetry: a matter of life and death. *Annu Rev Physiol* 65: 701–734, 2003
- Bishop DG, Rutberg L, Samuelsson B. The chemical composition of the cytoplasmic membrane of *Bacillus subtilis*. *Eur J Biochem* 2: 448–453, 1967
- Bishop EA, Birmingham MAC. Lipid composition of Gram-negative bacteria, sensitive and resistant to streptomycin. *Antimicrobial Agents Chem* 4: 378–379, 1973
- Bloch K. Cholesterol: evolution of structure and function. In: Vance DE, Vance J ed, *Biochemistry of lipids and membranes*. Amsterdam: Elsevier Science Publishers, p 363–382, 1991
- Boman HG. Innate immunity and the normal microflora. *Immunol Rev* 173: 5–16, 2000
- Chi SW, Kim JS, Kim DH, Lee SH, Park YH, Han KH. Solution structure and membrane interaction mode of an antimicrobial peptide gaegurin 4. *Biochem Biophys Res Commun* 352: 592–597, 2007
- Clark DP, Durell S, Maloy WL, Zasloff M. Ranalexin: a novel antimicrobial peptide from bullfrog (*Rana catesbeiana*) skin, structurally related to bacterial antibiotic, polymyxin. *J Biol Chem* 269: 10849–10855, 1994
- Clejan S, Krulwich TA, Mondrus KR, Sept-Young D. Membrane lipid composition of obligately and facultatively alkaliphilic strains of *Bacillus* spp. *J Bacteriol* 168: 334–340, 1986
- Conlon JM. Reflections on a systematic nomenclature for antimicrobial peptides from the skins of frogs of the family Ranidae. *Peptides* 29: 1815–1819, 2008
- Cronan JE, Roy-Vagelos P. Metabolism and function of the membrane phospholipids of *Escherichia coli*. *Biochim Biophys Acta* 165: 379–387, 1972
- Daleke DL. Regulation of phospholipid asymmetry in the erythrocyte membrane. *Curr Opin Hematol* 15: 191–195, 2008
- Dathé M, Schumann M, Wieprecht T, Winkler A, Beyermann M, Krause E, Matsuzaki K, Murase O, Bienert M. Peptide helicity and membrane surface charge modulate the balance of electrostatic and hydrophobic interactions with lipid bilayers and biological membranes. *Biochemistry* 35: 12612–12622, 1996
- Dowhan W. Molecular basis for membrane phospholipid diversity: why are there so many lipids? *Ann Rev Biochem* 66: 199–232, 1997
- Eun SY, Jang HK, Han SK, Ryu PD, Lee BJ, Han KH, Kim SJ. A helix-induced oligomeric transition of gaegurin 4, an antimicrobial peptide isolated from a Korean frog. *Mol Cells* 21: 229–236, 2006
- Gennis RB. The structure and composition of biomembranes. In: Gennis RB ed, *Biomembranes, molecular structure and functions*. New York: Springer Verlag, p 1–35, 1991
- Gidalevitz D, Ishitsuka Y, Muresan AS, Konovalov O, Waring AJ, Lehrer RI, Lee KY. Interaction of antimicrobial peptide protegrin with biomembranes. *Proc Natl Acad Sci USA* 100: 6302–6307, 2003
- Kagan B, Selsted ME, Ganz T, Lehrer RI. Antimicrobial defensins peptides form voltage-dependent ion-permeable channels in planar lipid bilayer membranes. *Proc Natl Acad Sci USA* 87: 210–214, 1990
- Kim HJ, Han SK, Park JB, Baek HJ, Lee BJ, Ryu PD. Gaegurin

- 4, a peptide antibiotic of frog skin, forms voltage-dependent channels in planar lipid bilayers. *J Pept Res* 53: 1–7, 1999
- Kim HJ, Kim SS, Lee MH, Lee BJ, Ryu PD. Role of C-terminal heptapeptide in pore-forming activity of antimicrobial agent, gaegurin 4. *J Pept Res* 64: 151–158, 2004
- Kim KS, Fulton RW. Ultrastructure of *Datura stramonium* infected with an euphorbia virus suggestive of witefly-transmitted geminivirus. *Phytopathology* 74: 236–241, 1984
- Lau YH, Caswell AH, Brunschwig J, Baerwald RJ, Garcia M. Lipid analysis and freeze-fracture studies on isolated transverse tubules and sarcoplasmic reticulum subfractions of skeletal muscle. *J Biol Chem* 254: 540–546, 1979
- Matsumoto K, Kusaka J, Nishibori A, Hara H. Lipid domains in bacterial membranes. *Mol Microbiol* 61: 1110–1117, 2006
- Matsuzaki K. Why and how are peptide-lipid interactions utilized for self-defense? Magainins and tachyplesins as archetypes. *Biochim Biophys Acta* 1462: 1–10, 1999
- Matsuzaki K. Control of cell selectivity of antimicrobial peptides. *Biochim Biophys Acta* (In press).
- Matsuzaki K, Harada M, Handa T, Funakoshi S, Fujii N, Yajima H, Miyajima K. Magainin 1-induced leakage of entrapped calcein out of negatively-charged lipid vesicles. *Biochim Biophys Acta* 981: 130–134, 1989
- Matsuzaki K, Sugishita K, Fujii N, Miyajima K. Molecular basis for membrane selectivity of an antimicrobial peptide, magainin 2. *Biochemistry* 34: 3423–3429, 1995
- Morein S, Andersson AS, Rilfors L, Lindblom G. Wild-type *Escherichia coli* cells regulate the membrane lipid composition in a “Window” between gel and non-lamellar structures. *J Biol Chem* 271: 6801–6809, 1996
- Morikawa N, Hagiwara K, Nakajima T. Brevinin-1 and brevinin-2, unique antimicrobial peptides from the skin of the frog *Rana brevipoda porsa*. *Biochem Biophys Res Comm* 189: 184–190, 1992
- Orlov DS, Nguyen T, Lehrer RI. Potassium release, a useful tool for studying antimicrobial peptides. *Microbiol Methods* 49: 325–328, 2002
- Park JB, Kim HJ, Ryu PD, Moczydlowski E. Effect of phosphatidylserine on unitary conductance and  $\text{Ba}^{2+}$  block of the BK  $\text{Ca}^{2+}$ -activated  $\text{K}^+$  channel: re-examination of the surface charge hypothesis. *J Gen Physiol* 121: 375–398, 2003
- Park S, Son WS, Kim YJ, Kwon AR, Lee BJ. NMR spectroscopic assessment of the structure and dynamic properties of an amphibian antimicrobial peptide (Gaegurin 4) bound to SDS micelles. *J Biochem Mol Biol* 40: 261–269, 2007
- Park SH, Kim YK, Park JW, Lee BJ, Lee BJ. Solution structure of the antimicrobial peptide gaegurin 4 1H and 15N nuclear magnetic resonance spectroscopy. *Eur J Biochem* 267: 2695–2704, 2000
- Park JM, Jung JE, Lee BJ. Antimicrobial peptides from the skin of a Korean frog, *Rana rugosa*. *Biochem Biophys Res Comm* 205: 948–954, 1994
- Shai Y. From innate immunity to de-novo designed antimicrobial peptides. *Curr Pharm Des* 8: 715–725, 2002
- Simmaco M, Mignogna G, Barra D, Bossa F. Novel antimicrobial peptides from skin secretion of the European frog, *Rana esculenta*. *FEBA Lett* 324: 159–161, 1993
- Won HS, Kang SJ, Lee BJ. Action mechanism and structural requirements of the antimicrobial peptides, gaegurins. *Biochim Biophys Acta* 2009 (In press).
- Zasloff M. Antimicrobial peptides of multicellular organisms. *Nature* 415: 389–395, 2002